Multi-Input/Multi-Output Controller Design for Longitudinal Decoupled Aircraft Motion

J.L. Speyer,* J.E. White,† R. Douglas,‡ and D.G. Hull*
The University of Texas, Austin, Texas

For the AFTI/F-16 aircraft a multi-input/multi-output controller design is described which decouples pitch rate and normal acceleration. A controllable state space is determined which forms the model used by the linear quadratic Gaussian synthesis technique. The dynamic model guarantees zero steady-state tracking, and the LQG synthesis technique produces the compensator structures with theoretical robustness guarantees. To ensure that the nominal system remains robust with respect to model and parameter uncertainties, singular value analysis is used. A combination of symmetric root locus, time response, and singular value analysis is used to describe the performance of the design.

I. Introduction

THE development of design techniques for multi-input/multi-output (MIMO) linear systems has been an active area of research over the last few years.[1] In particular, the development of robust controllers based upon classical gain and phase margin criteria has been pursued in Refs. 2-4. These works extend the single-input/single-output results of Ref. 5 for the phase and gain margin of the linear-quadratic regulator (LQR) to the MIMO LQR. These important gain and phase margin results assume full-state feedback. If some of the feedback states are not available, they may be deduced from an observer (or filter). However, the guaranteed gain and phase margin results of the LQR[2,3] may decrease markedly when the observer is included. Doyle and Stein[6] show that the proper choice of the observer gains allows the guaranteed gain and phase results of the full-state feedback LQR to be obtained asymptotically.

This approach to robust controller synthesis is applied to the design of the AFTI/F-16 aircraft longitudinal autopilot for decoupling the pitch rate and normal acceleration where step functions in pitch rate and acceleration are to be tracked. For example, in the pitch pointing mode, pitch rate is to be tracked with minimal transient disturbance. The AFTI/F-16 control system development concepts and design are found in Ref. 16, and in particular, LQR application to the various AFTI/F-16 control modes is given in Ref. 17. This includes some earlier results of the work given here.

A major design issue is the determination of the state space on which the LQR synthesis technique is to be applied. This aspect of the design technique is similar to the development of compensator design in classical single-input/single-output (SISO) synthesis.[7] A controllable state space is chosen so that *all* of the states and controls that are used in the LQ problem have a zero steady-state equilibrium. With this state space the infinite time quadratic performance index is well behaved, the robustness properties for the full state feedback regulator[2,3] apply, and the resulting controller will have zero steady-state errors in the presence of parameter uncertainty. This is because integral compensation is introduced by this state space.[7]

However, in the AFTI/F-16 longitudinal decoupling problem, a state space which produces integral compensation for both the errors in acceleration and pitch rate is *not* controllable. A controllable state space is determined by reducing the order of the state space by using a particular linear combination of the state variables. LQR synthesis is applied to this final state space.

All of the states are not measured. In fact, the only assumed measurements are normal acceleration, pitch rate, and angle of attack. An observer is designed to estimate the required actuator states, since there are no measurements on any of the elevator or flap states. The design procedure is divided into two parts. First, the weightings on the states in the LQR synthesis are chosen so that the system response remains slow relative to the higher-order actuator dynamics. This allows a reduced-order controller and alleviates the need to estimate the higher-order actuator states. Second, the observer is designed to capture the full feedback results of LQR synthesis. By using the suggestion of Doyle and Stein,[6] the observer weightings are chosen so that the full-state feedback transfer function is obtained asymptotically. Impressive robust response is obtained for large parameter variations. This robustness is evaluated by using singular value techniques. The singular values of the error models due to parameter variations and the higher-order actuators are derived and plotted on the singular value frequency charts. The gap between the singular values of the nominal inverse return difference matrix and the largest singular value of the error models guarantees stability. Time responses, which include the higher-order actuator dynamics and parameter variations, are also displayed to ensure that the desired transient response is obtained.

II. System Dynamics

A. Plant Model

The linear, longitudinal equations of perturbed motion about straight and level flight are written here in the simplified form

$$\dot{\alpha} = Z_\alpha \alpha + Z_q q + Z_e e + Z_f f \tag{1}$$

$$\dot{q} = M_\alpha \alpha + M_q q + M_e e + M_f f \tag{2}$$

where α is the perturbed angle of attack, q is the perturbed pitch rate, e is the perturbed elevator deflection, and f is the perturbed flap deflection. The longitudinal stability derivatives $(Z_\alpha, Z_q, Z_e, Z_f, M_\alpha, M_q, M_e, M_f)$ are assumed known. These equations use the simplifying assumption that the stability

Presented as Paper 81-1839 at the AIAA Guidance and Control Conference, Albuquerque, N.M., Aug. 19-21, 1981; submitted Sept. 30, 1981; revision received Nov. 16, 1983.

*Professor, Department of Aerospace Engineering and Engineering Mechanics. Associate Fellow AIAA.

†Research Assistant, Department of Aerospace Engineering and Engineering Mechanics. Member AIAA.

‡Research Assistant, Department of Aerospace Engineering and Engineering Mechanics. Student Member AIAA.

derivatives associated with the perturbed forward velocity are negligible.

The normal acceleration experienced by the accelerometer is composed of the acceleration of the center of mass and the acceleration relative to the center of mass given as the sum

$$A = \beta_1 (q - \dot{\alpha}) + \beta_2 \dot{q} \tag{3}$$

where

$$\beta_1 \triangleq \frac{2\pi U}{360\, g}, \qquad \beta_2 \triangleq \frac{2\pi x_{\text{acc}}}{360\, g} \tag{4}$$

where U is aircraft velocity, g is the acceleration of gravity, and x_{acc} is the distance from the center of mass to the accelerometer.

The actuator dynamics are modeled as a third-order linear system

$$\dot{e} = e_1, \quad \dot{e}_1 = e_2, \quad \dot{f} = f_1, \quad \dot{f}_1 = f_2 \tag{5}$$

$$\dot{e}_2 = -H_1 e_2 - H_2 e_1 - H_3 e + H_4 u_e \tag{6}$$

$$\dot{f}_2 = -H_5 f_2 - H_6 f_1 - H_7 f + H_8 u_f \tag{7}$$

The inputs to the elevator and flap actuators are the controls u_e and u_f, respectively. Numerical subscripts on the state variables denote time differentiation unless otherwise defined.

B. Change of Plant Model States

The choice of command inputs for modal decoupling is a critical design consideration. The command set of A and q was chosen in our design because these quantities are most versatile for the various mission requirements.[16,17] This choice is far more stringent than other possible choices, such as commanding step inputs for the pitch attitude, θ, and α as chosen in Ref. 4. In Ref. 4, step inputs result in steady-state control surface deflections, whereas here step inputs on (A, q) result in ramping control surface deflections, as is shown below.

Since (A, q) are chosen to be the command inputs, it is rather natural to use A and q as the state variables rather than (α, q). By using Eqs. (1-3), the dynamic equations become

$$\dot{A} = D_A A + D_q q + D_e e + D_f f + \Omega_e e_1 + \Omega_f f_1 \tag{8}$$

$$\dot{q} = H_A A + H_q q + H_e e + H_f f \tag{9}$$

where

$$D_A \triangleq Z_\alpha + \frac{M_\alpha \Omega_q}{\Omega_\alpha} \tag{10}$$

$$D_s \triangleq Z_s \Omega_\alpha - Z_\alpha \Omega_s + M_s \Omega_q - \frac{M_\alpha \Omega_q \Omega_s}{\Omega_\alpha}; \qquad s = q, e, f \tag{11}$$

$$H_A \triangleq \frac{M_\alpha}{\Omega_\alpha}, \quad H_s \triangleq M_s - \frac{M_\alpha \Omega_s}{\Omega_\alpha}; \qquad s = q, e, f \tag{12}$$

$$\Omega_s \triangleq \beta_2 M_s - \beta_1 Z_s + \beta_1 \delta_{s,q}; \qquad s = \alpha, q, e, f \tag{13}$$

where $\delta_{s,q} = 1$ if $s = q$ and zero otherwise.

Physically, acceleration and pitch rate cannot be held in steady state by constant deflections of the elevator and flap. For example, if $A = 0$ and $q = 1$ deg/s, then the flap must constantly change to null out the acceleration induced by the increasing angle of attack. This is shown mathematically by noting that

$$\det \begin{vmatrix} D_e & D_f \\ H_e & H_f \end{vmatrix} = 0 \tag{14}$$

regardless of the values of the stability derivatives. Nonzero values of e_1 and f_1 are required to keep A and q at nonzero constant values.

III. State Space Design and Linear-Quadratic Regulator Synthesis

A. State Space for LQR Synthesis Design

The choice of state space for LQR synthesis is one which has zero steady-state error. The zero steady-state tracking error should be insensitive to parameter variations.[7] The tracking errors are defined as

$$E_A \triangleq A_{CT} - A, \qquad E_q \triangleq q_{CT} - q \tag{15}$$

where A_{CT} and q_{CT} are the outputs of first-order lags. These prefilters, which are used to smooth the transient responses of the autopilot, are expressed as

$$\dot{A}_{CT} = -\omega_A A_{CT} + \omega_A A_C \tag{16}$$

$$\dot{q}_{CT} = -\omega_G q_{CT} + \omega_G q_C \tag{17}$$

where A_C and q_C are the constant step input commands from the pilot. The inclusion of these lags into the LQR synthesis design does not cause any difficulty.

If E_A and E_q are differentiated with respect to time, the resulting differential equations have biases due to the input commands A_C and q_C. The coefficients of A_C and q_C are parameter sensitive; therefore, the steady-state errors are parameter sensitive. See Ref. 7 where this is demonstrated for a simple example. Furthermore, e_1 and f_1 and therefore u_e and u_f are states and controls which, as shown above, cannot be zero in steady state for arbitrary A_C or q_C. If u_e and u_f are weighted in a quadratic cost, the resulting LQR controller will *not* result in zero steady-state error.[7] By extending Athans' suggestion,[7] E_A and E_q are differentiated once more. Then

$$\dot{E}_A = E_{A_1}, \qquad \dot{E}_q = E_{q_1} \tag{18}$$

$$\dot{E}_{A_1} = D_A E_{A_1} + D_q E_{q_1} - D_A A_{CT_1} - D_q q_{CT_1} - \omega_A A_{CT_1} - D_e e_1 - D_f f_1 - \Omega_e e_2 - \Omega_f f_2 \tag{19}$$

$$\dot{E}_{q_1} = H_A E_{A_1} + H_q E_{q_1} - H_A A_{CT_1} - H_q q_{CT_1} - H_e e_1 - H_f f_1 - \omega_G q_{CT} \tag{20}$$

The actuator dynamics given in Eqs. (5-7) and the prefilters in Eqs. (16) and (17) are all differentiated once where now $\dot{u}_e$ and $\dot{u}_f$ become the control variables.

Two difficulties occur here. First, unlike the simple example of Ref. 7, all the states and controls still do not go to zero in steady state. For nonzero A_C and q_C, e_1 and f_1, and, therefore, $\dot{u}_e$ and $\dot{u}_f$, are nonzero in steady state. If $\dot{u}_e$ and $\dot{u}_f$ are weighted in a quadratic cost, the resulting LQR controller will still not result in zero steady-state error.

Another difficulty is that the state space of $[E_A, E_{A_1}, E_q, E_{q_1}, e_1, e_2, e_3, f_1, f_2, f_3]$ is not controllable (or stabilizable) with respect to $[\dot{u}_e, \dot{u}_f]$. Consider the original state space of (α, q) where

$$\dot{E}_A = \dot{A}_{CT} - \dot{A} = \dot{A}_{CT} - [\beta_1 (\dot{q} - \ddot{\alpha}(\dot{\alpha}, \dot{q}, \dot{f}, \dot{e})) + \beta_2 \ddot{q}(\dot{\alpha}, \dot{q}, \dot{f}, \dot{e})] \tag{21}$$

$$\dot{E}_q = \dot{q}_{CT} - \dot{q} \tag{22}$$

Note that $\ddot{\alpha}$ and $\ddot{q}$ are related to the state variables through their differential equations. Also, $\dot{A}_{CT}$ and $\dot{q}_{CT}$ are not controllable (although stabilizable), so their integration does not contribute to the controllable state space. Therefore, integrat-

ing $\dot{E}_A$ and $\dot{E}_q$ gives

$$E_A = A_{CT} - [\beta_1(q - \dot{\alpha}) + \beta_2 \dot{q}] \tag{23}$$

$$E_q = q_{CT} - q \tag{24}$$

These two integrations produce only *one* new controllable variable, q.

From Eq. (21) and after some manipulation, the state E_{A_1} can be eliminated by the linear combination

$$-E_{A_1} = Kq_1 - (D_A - KH_A)E_A - \Omega_\alpha E_q + \Omega_e e_1 + \Omega_f f_1 - A_{CT_1}$$
$$-[(D_A - KH_A)/\omega_A]A_{CT_1} - \frac{\Omega_\alpha}{\omega_G} q_{CT_1}$$
$$+(D_A - KH_A)A_C + \Omega_\alpha q_C \tag{25}$$

where $K \triangleq D_e/H_e = D_f/H_f$, see Eq. (14). If Eq. (25) is introduced into Eqs. (18-20), then the controllable state space is $[E_A, E_q, E_{q_1}, e_1, e_2, e_3, f_1, f_2, f_3]$. Note that constant forcing terms due to A_C and q_C reappear in the dynamics.

The above suggests that additional differentiations be applied to the dynamic system associated with the controllable state space. The dynamic system for LQR synthesis becomes

$$\dot{E}_A = E_{A_1}, \qquad \dot{E}_q = E_{q_1}, \qquad \dot{E}_{q_1} = q_{CT_2} - q_2 \tag{26}$$

$$\dot{E}_{A_1} = [1 + (D_A - KH_A)/\omega_A]A_{CT_2} - Kq_2 + (D_A - KH_A)E_{A_1}$$
$$+\Omega_\alpha E_{q_1} - \Omega_e e_2 - \Omega_f f_2 + (\Omega_\alpha/\omega_G) q_{CT_2} \tag{27}$$

$$\dot{q}_2 = H_A(A_{CT_2} - \dot{E}_{A_1}) + H_q q_2 + H_e e_2 + H_f f_2 \tag{28}$$

The actuator dynamics given in Eqs. (5-7) and the prefilters in Eqs. (16) and (17) are all differentiated *twice* where now $v = [v_e, v_f] \triangleq [\ddot{u}_e, \ddot{u}_f]$ becomes the control vector. The final stabilizable state space is

$$x_R^T \triangleq [E_A, E_q, E_{A_1}, E_{q_1}, q_2, e_2, e_3, e_4, f_2, f_3, f_4, A_{CT_2}, q_{CT_2}] \tag{29}$$

Note that all the states and controls go to zero in steady state for step input commands. This procedure ensures that the resulting LQR controller has sufficient integral compensation to produce zero steady-state tracking in the presence of all parameter uncertainty for which the controller remains stable. The compensation structure is determined by the state space x_R but mechanized by the double integration of x_R. This is because the double integration required for the actuator inputs cancels the double differentiation of the plant output required to produce the state x_R.

B. Linear Quadratic Regulator Synthesis Procedure

The LQR synthesis problem is that of determining the control v which minimizes the performance index

$$J = \frac{1}{2}\int_0^\infty (x_R^T Q x_R + v^T R v)\, dt \tag{30}$$

where $R > 0$ and $Q \geq 0$, subject to the dynamic equation

$$\dot{x}_R = F_R x_R + B_R v \tag{31}$$

where the F_R and B_R matrices can be identified from the previous section. The solution to this problem is a linear controller of the form

$$v = -R^{-1}B_R^T P x_R = G_R x_R \tag{32}$$

where P satisfies the algebraic matrix Riccati equation.[8,9] The constant gains are determined from the Stanford Discrete LQR Synthesis Program, which allows the input to be in continuous or discrete form. Although the above formulation is stated in continuous time, our simulation results are based upon determining the discrete form of Eq. (31) and the associated discrete gains for a given sample rate. The compensator, given in Fig. 1 for full-state feedback, involves proportional and integral elements; no differentiation is required except in forming the actuator states. This full-state compensator design requires that 26 gains be calculated from the LQR synthesis procedure by inputting the values of the symmetric weighting matrices Q and R. In the next section,

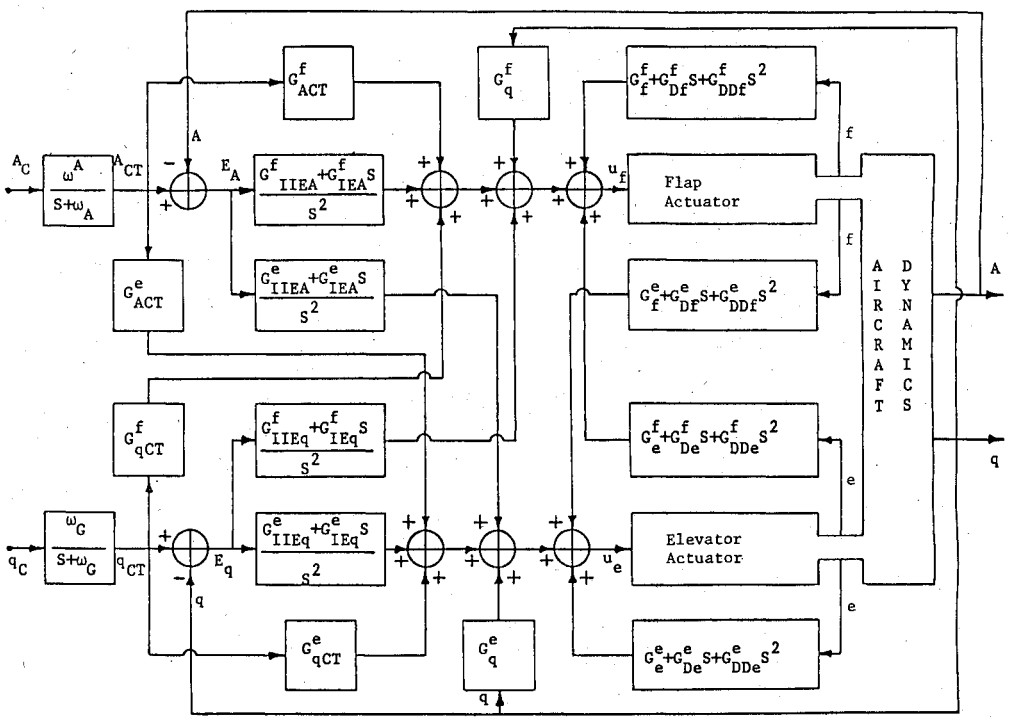

Fig. 1 Full feedback LQR compensator.

the weightings in the cost criteria are chosen so that the gains associated with the higher-order actuator states can be neglected.

C. Choice of LQR Synthesis Weightings

Since pitch rate, normal acceleration, and angle of attack are the only assumed measurements, the actuator states must be estimated. Therefore, the control gains should be chosen so that precise dependence on the actuator states is avoided if possible. The weightings are chosen so that a reasonable degree of decoupled motion is obtained without stimulating the higher-order actuator dynamics. The following discussion develops the method for determining the LQR weightings: First, diagonal weightings are placed on the states E_A, E_q, E_{A_I}, and E_{q_I}, and R is the identity matrix. The weights on E_{A_I} and E_{q_I} tend to reduce the transient response overshoot. However, by constructing the symmetric root locus[5,10] generated by changing a parameter ρ which multiplies Q, it is noted that a root on the real axis emanating from the first-order actuator dynamics moves significantly to the left. Furthermore, a noticeable movement of the higher-order actuator roots occurs with increasing ρ. This increase in bandwidth does not allow stability without the higher-order actuator feedbacks. Second, consider weightings only on the terms E_A^2, E_q^2, and $E_A E_q$. Some reduction of the transient response overshoot is obtained by the off-diagonal weighting terms. Interestingly, the fast real-axis closed-loop pole emanating from the first-order pole of the actuators does not occur for the same range of values of ρ. Furthermore, the closed-loop poles associated with the higher-order dynamics hardly move for the same range of values of ρ. For $\rho = 1$, removing the feedbacks associated with the higher-order actuator states (i.e., for $G_{De} = G_{DDe} = G_{Df} = G_{DDf} = 0$ in Fig. 1) does not noticeably change the system response in a simulation that includes the higher-order actuator modes, even for sizeable system parameter variations. This robustness is characterized in Sec. V by appealing to singular value analysis. Therefore, since only the first-order actuator states of elevator and flap deflection need be fed back, the estimator in the following section is designed by neglecting the fast actuator dynamics, thereby reducing the computational burden.

IV. State Observer/Kalman Estimator Design

Direct measurements of the flap and elevator deflections are assumed not to be available and must be determined from the available measurements of acceleration and pitch rate (angle of attack measurements are available but are not used in this study since they are relatively noisy). The design of observers and Kalman estimators is well known.[5,11] Our emphasis is on the design of observers which enhance overall system robustness in the presence of parameter uncertainty. The observer is chosen so that the open-loop transfer function, determined by cutting the loop at the inputs to the actuators, asymptotically becomes that of the full-state feedback system.[6] Given the results of Refs. 2 and 3, robust behavior is expected.

The observer design is based on the observable states and known inputs as

$$\underline{x}^T \triangleq [A, q, e, f], \qquad u^T \triangleq [u_e, u_f] \tag{33}$$

and the measurement z is a noisy observation of A and q as

$$z \triangleq \underline{C}\underline{x} + \nu \tag{34}$$

where $\underline{C} = [I, 0]$ is a 2×4 matrix when acceleration and pitch rate measurements are available, and ν is an assumed white noise measurement process with zero mean and power spectral density

$$V \triangleq \begin{bmatrix} V_A & 0 \\ 0 & V_q \end{bmatrix} = \begin{bmatrix} 5.81 \times 10^{-5}(\text{g})^2\text{s} & 0 \\ 0 & 1.006 \times 10^{-4}\ \text{deg}^2/\text{s} \end{bmatrix} \tag{35}$$

The angle of attack probe has a power spectral density of 2.0521×10^{-2} deg^2-s and is sufficiently noisy to be neglected in favor of the more accurate pitch rate gyro and accelerometer measurements. These values have been obtained from Ref. 12. The observer is designed using the dynamic system

$$\dot{\underline{x}} = \underline{F}\underline{x} + \underline{B}u + w \tag{36}$$

where

$$\underline{F} \triangleq \begin{bmatrix} D_A & D_q & (D_e - \Omega_e H_9) & (D_f - \Omega_f H_{11}) \\ H_A & H_q & H_e & H_f \\ 0 & 0 & -H_9 & 0 \\ 0 & 0 & 0 & -H_{11} \end{bmatrix}$$

$$\underline{B} \triangleq \begin{bmatrix} \Omega_e H_{10} & \Omega_f H_{12} \\ 0 & 0 \\ H_{10} & 0 \\ 0 & H_{12} \end{bmatrix} \tag{37}$$

where the two actuators are modeled as first-order lags with associated parameters $(H_9, H_{10}, H_{11}, H_{12})$ and where w is theoretically a white noise process in the usual Kalman filter formulation with assumed zero mean and power spectral density W. However, as a design technique, W is chosen larger than the underlying stochastic process noise to accommodate uncertainties in the system parameters.[13] Usually, this is done by increasing the diagonal elements of W. An improved approach is that suggested by Doyle and Stein,[6] whereby the gains are chosen so that the full-state feedback robustness results are obtained asymptotically.

The compensator obtained by combining the observer and controller is obtained by using a state vector (for simplicity, the prefilter states are ignored below) composed of the constructed states used in the compensator, $x_C^T = [\int\int E_A\,dt, \int\int E_q\,dt, \int E_A\,dt, \int E_q\,dt]$, and the observable states $\underline{x}$. The state space used for describing the compensator is $x^T \triangleq [x_C^T, \underline{x}^T]$. The estimator is then of the form ($\hat{x}$ is the estimated value of the state x)

$$\dot{\hat{x}} = (F + BK_C - K_f C)\hat{x} + K_f z \tag{38}$$

where

$$B = \begin{bmatrix} 0 \\ \cdots \\ \underline{B} \end{bmatrix}, \qquad K_f = \begin{bmatrix} 0 \\ \cdots \\ \underline{K}_f \end{bmatrix}, \qquad C = \left[0 \;\vdots\; \underline{C}\right] \tag{39}$$

$$F = \left[\begin{array}{c|c} \Lambda & -\Lambda^T \\ \hline 0 & \underline{F} \end{array}\right], \qquad \Lambda \triangleq \left[\begin{array}{c|c} 0 & I_2 \\ \hline 0 & 0 \end{array}\right] \tag{40}$$

where $\underline{K}_f$ is the observer gain and K_C is the controller gain composed of G_R, see Eq. (32), and an additional zero column which operates on the estimate of A. (Note that because of the controllability problem A is fed back only to form the constructed states used for integral compensation.)

The open-loop transfer matrix obtained by breaking the loop at the plant input is

$$K(S)G_p(S) = K_C\left[SI - F - BK_C + K_fC\right]^{-1} \times K_fC[SI - F]^{-1}B \tag{41}$$

where the plant transfer matrix is

$$G_p(S) = C[SI - F]^{-1}B = \underline{C}[SI - \underline{F}]^{-1}\underline{B} \tag{42}$$

and $K(S)$ is the compensator transfer matrix.

In Ref. 6 it is shown that if the process noise power spectral density (psd) used to form the Kalman gain K_f is chosen as

$$W = W_0 + \beta^2 BUB^T \tag{43}$$

where U is a 2×2 positive definite matrix, $W_0 \geq 0$ is a known noise psd, and β is a design parameter, then as $\beta \to \infty$ the observer gain becomes

$$K_f \cong \beta BU^{\frac{1}{2}}V^{-\frac{1}{2}} \tag{44}$$

and

$$K(S)G_p(S) \cong K_C[SI - F]^{-1}B = G_R[SI - F_R]^{-1}B_R \tag{45}$$

which is the loop transfer matrix for the full-state feedback LQ regulator. This result holds for the present problem, since $G_p(S)$ is minimal phase. (Actually, there are no transmission zeros.)

V. Robustness and Singular Value Analysis

The LQR has been shown in Refs. 2 and 3 to have important robustness properties. In particular, for a diagonal error model (no assumed coupling between channels), the LQR has simultaneously in each feedback loop a guaranteed minimum gain margin of $(\frac{1}{2}, \infty)$ *or* a guaranteed minimum phase margin of ± 60 deg. A slight generalization of this result is given in Ref. 14. This inherent robustness property of the LQR is asymptotically obtained by the linear quadratic Gaussian (LQG) regulator by designing the observer/filter as suggested in Sec. IV.

This absolute robustness property is associated with the nominal system. To assess robustness relative to parameter variations and neglected dynamics, singular value analysis is helpful. Whereas in SISO analysis phase and gain margin are measures of the closeness of the Nyquist plot to the $(-1, 0)$ point, singular value analysis measures this distance in the MIMO system in terms of the singularity of a matrix. The matrix which is of most concern here is the inverse return difference matrix

$$T(S) = I + \left(K(S)G_p(S)\right)^{-1} \tag{46}$$

The central robustness relation[6] (which guarantees that the matrix $(T + L)$ does not lose rank) is that

$$\underline{\sigma}(T(\omega)) > \bar{\sigma}(L(\omega)) \text{ for all frequencies } \omega \tag{47}$$

where the smallest singular value $\underline{\sigma}$ and the largest singular value $\bar{\sigma}$ are found from the respective square roots of the eigenvalues of the Hermitian matrix, i.e., $T(-\omega)^T T(\omega)$ or $L(-\omega)^T L(\omega)$. $L(\omega)$ is a multiplicative error model, since if $G_p(S)$ is the nominal plant, then the perturbed plant $G_p'(S)$ is expressed as

$$G_p'(S) = G_p(S)[I + L(S)] \tag{48}$$

If condition (47) is satisfied, then stability is guaranteed.[6]

The construction of these error models is important in order to evaluate robustness. Of most concern in this study is the effect of the neglected higher-order actuator dynamics and system parameter variations on stability. The error model for the actuators[15] is obtained by considering the first-order actuator model to be the nominal, i.e. $G_A(S) = \text{Diag}[\omega_A/(S + \omega_A)]$, and the perturbed actuator plant to be $G_A'(S) = \text{Diag}[\omega_A^2/(S^2 + 2\xi\omega_A S + \omega_A^2)]G_A(S)$. Substitution into condition (48) yields $L_A(S) = \text{Diag}[(G_A'/G_A) - I]$. Since both diagonal elements are the same

$$\bar{\sigma}(L_A(\omega)) = \left| \frac{S^2 + 2\xi\omega_A S}{S^2 + 2\xi\omega_A S + \omega_A^2} \right|_{S=j\omega} \tag{49}$$

The error model associated with parameter variations is derived in an elegant form by using a matrix identity. For simplicity define $\psi(S) \triangleq (SI - F)^{-1}$. If a parameter varies it can affect both the F and B matrices. Denote these perturbations away from the nominal F and B as ΔF and ΔB, respectively. The perturbed plant under parameter variation is

$$G_p' = C\left[\psi^{-1} + \Delta F\right]^{-1}(B - \Delta B) \triangleq G_p\left[I + L_p\right] \tag{50}$$

By using the matrix inversion lemma[6]

$$\left(\psi^{-1} + \Delta F\right)^{-1} = \psi - \psi\Delta F(I + \psi\Delta F)^{-1}\psi \tag{51}$$

Eq. (50) becomes

$$G_p' = C\left[\psi - \psi\Delta F(I + \psi\Delta F)^{-1}\psi\right](B - \Delta B) \tag{52}$$

Since $G_p = C\psi B$, Eq. (50) using Eq. (52) produces the desired singular value as

$$\bar{\sigma}(L_p) = \bar{\sigma}\left\{G_p^{-1}C\psi\left[\Delta B + \Delta F(I + \psi\Delta F)^{-1}\psi B - \Delta F(I + \psi\Delta F)^{-1}\psi\Delta B\right]\right\} \tag{53}$$

These error models are used in the next section to evaluate robustness of the LQG regulator.

Table 1 Simulation input data

Parameters	
Actuator model	Prefilter, rad/s
$H_9 = H_{10} = H_{11} = H_{12} = 20$ $H_1 = H_5 = 92.8$ $H_2 = H_6 = 4160$ $H_3 = H_4 = H_7 = H_8 = 54{,}080$	$\omega_G = 5$ $\omega_A = 5$
Aerodynamic, flight conditions of Mach 0.9, 20,000 ft MSL	
$U = 933.15$ ft/s $\Delta x_{acc} = 14$ ft $Z_\alpha = -1.6187\ \text{s}^{-1}$ $Z_q = 0.997$ $Z_e = -0.16625\ \text{s}^{-1}$	$Z_f = -0.1904\ \text{s}^{-1}$ $M_\alpha = 2.9618\ \text{s}^{-2}$ $M_q = -0.7704\ \text{s}^{-1}$ $M_e = -22.5382\ \text{s}^{-2}$ $M_f = -4.2615\ \text{s}^{-2}$
Limits	
Flap ± 20 deg Elevator ± 25 deg	Flap rate ± 52 deg/s Elevator rate ± 60 deg/s
Miscellaneous constants	
$g = 32.2\ \text{ft/s}^{-2}$	

VI. System Performance

The properties of the longitudinal decoupled control system for the AFTI/F-16 are evaluated by use of singular values, which guarantee robustness, and the associated transient responses, which are obtained by a linear simulation. The nominal parameters used in the simulation and controller are given in Table 1. The LQR weightings are

$$Q = \left[\begin{array}{cc|c} 10^4 & -3\times10^3 & \\ -3\times10^3 & 4\times10^3 & 0 \\ \hline & 0 & 0 \end{array}\right], \qquad R = I_2 \qquad (54)$$

where I_j is a $j \times j$ identity matrix.

The nonzero weightings are on (E_A, E_q) of the state space for LQR design (Sec. III). The observer is designed with W given by Eq. (43) where $W_0 = 0.1$, $U = I_2$, and $\beta^2 = 0.25$. In Table 2, the gains for the controller and filter are given. The gains of both the observer and the filter are obtained using the discrete option of the Stanford LQR Synthesis Program. A sample time of $\frac{1}{64}$ s is used. The program converts the continuous system, Eq. (31), used in the determination of the controller gains, and the continuous system, Eq. (36), used in the determination of the observer gains, into a discrete form. The assumptions are that the inputs are constant over the sampling interval and the measurements are taken at each sample time. The measurement variance is obtained by dividing the power spectral density, Eq. (35), by the sample time as $V/0.01563$. It should be noted that the filter and controller are compatible, since the only states that are observable are those emanating from the observer. All the other controller states are constructed by additional integrations.

The higher-order actuator states are not fed back in the control scheme. The gains associated with these feedbacks (see Table 2) are quite small. Little difference is seen, either if the higher-order actuator dynamics are included in the LQR design and then the feedbacks ignored, or if the higher-order actuator dynamics are ignored in the LQR design. Furthermore, the responses for the full-state feedback, the reduced feedback, and the reduced feedback controller with observer are almost identical in the simulation where the higher-order actuator dynamics are included. The presence of the prefilter helps somewhat in reducing the overshoot. The off-diagonal weighting has an important effect on the pitch rate response and a much smaller effect on the acceleration response. The value of -3000 in Eq. (54) gives good pitch rate response in the pointing mode and a reasonable oscillatory response in the translation mode (nonzero acceleration command and zero pitch rate command).

Table 2 Baseline regulator and filter gains

Regulator baseline gains	
$G_q^e = 1.5666$	$G_q^f = 0.3782$
$G_{IIEA}^e = -9.9458$	$G_{IIEA}^f = 97.3667$
$G_{IEA}^e = -7.2114$	$G_{IEA}^f = 35.3897$
$G_{IIEq}^e = -44.0637$	$G_{IIEq}^f = -32.8069$
$G_{IEq}^e = -13.2858$	$G_{IEq}^f = -2.3989$
$G_e^e = -1.8272$	$G_e^f = -0.2799$
$G_{De}^e = -0.3647$	$G_{De}^f = -5.5982 \times 10^{-3}$
$G_{DDe}^e = -3.5409 \times 10^{-4}$	$G_{DDe}^f = -5.4282 \times 10^{-5}$
$G_f^e = -0.2979$	$G_f^f = -0.2571$
$G_{Df}^e = -5.8222 \times 10^{-3}$	$G_{Df}^f = -5.5444 \times 10^{-3}$
$G_{DDf}^e = -5.526 \times 10^{-5}$	$G_{DDf}^f = -5.7886 \times 10^{-5}$
$G_{ACT}^e = -0.8448$	$G_{ACT}^f = 3.6138$
$G_{qCT}^e = -1.4474$	$G_{qCT}^f = 0.6065$

Filter baseline gains with A, q measurements	
$K_{AA} = 0.8017$	$K_{qA} = 0.02971$
$K_{Aq} = 0.05145$	$K_{qq} = 0.9376$
$K_{Ae} = -3.1333$	$K_{qe} = -2.1064$
$K_{Af} = 4.1359$	$K_{qf} = -1.5053$

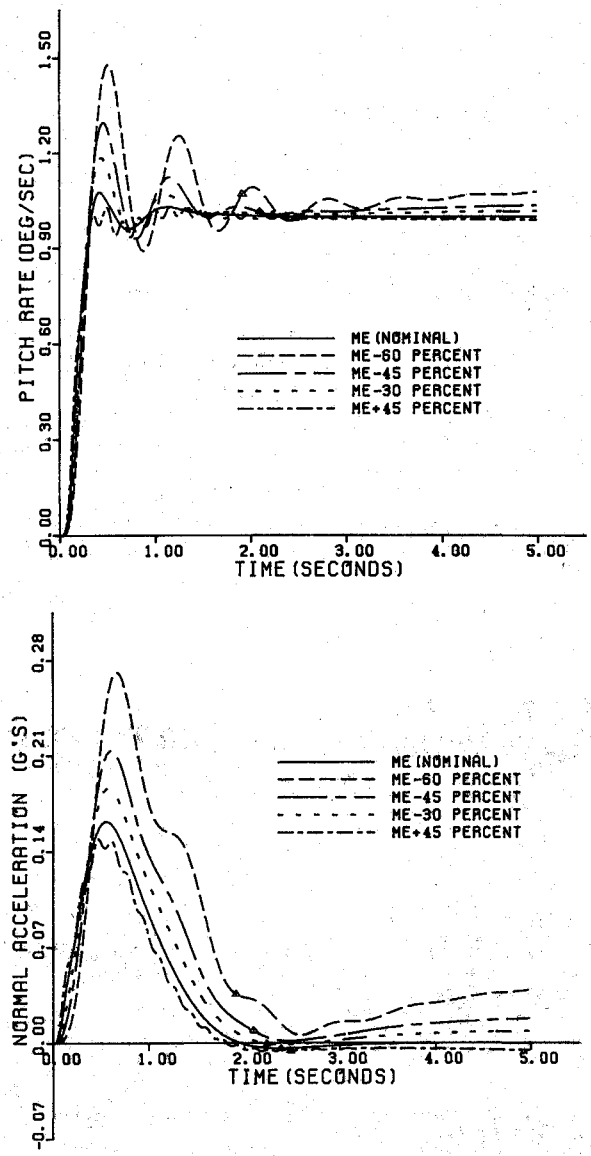

Fig. 2 M_e variations, baseline A,q observer.

The essence of good control system design is its response in the presence of parameter uncertainty. The most sensitive parameter (and the one varied in the following study) seems to be the moment coefficient due to elevator deflection, M_e. Figures 2a and 2b give the pointing mode response as M_e is changed from $+45\%$ to -60%. A mark on all curves indicates where the flap limit is reached. These time responses are to be contrasted with the singular value analysis.

The singular value plots of the plant, the open-loop transfer matrix, and inverse return difference matrix give additional insight into the system properties and robust stability of the LQG design. Figure 3 shows both the maximum ($\bar{\sigma}$) and minimum ($\underline{\sigma}$) singular values for the plant transfer matrix, Eq. (42), where the inputs are applied to the first-order actuator model of elevator and flap, and the outputs are acceleration and pitch rate. Note that at low frequencies the smallest singular value behaves as a differentiation.

The singular values associated with the open-loop transfer matrix, Eq. (41), (loop broken at the plant input) associated with the full-state feedback LQ regulator are shown in Fig. 4 with $\beta = \infty$. Here the smaller singular value behaves almost as an integrator over all frequencies. The largest singular value,

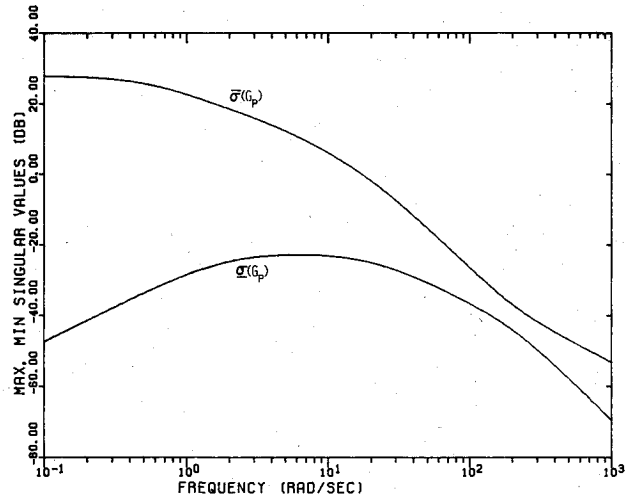

Fig. 3 Singular values of plant transfer matrix.

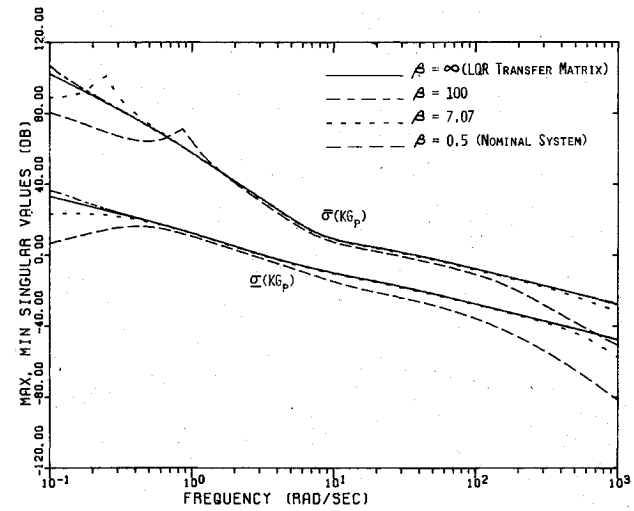

Fig. 4 Singular values of loop transfer matrix showing full-state loop transfer recovery.

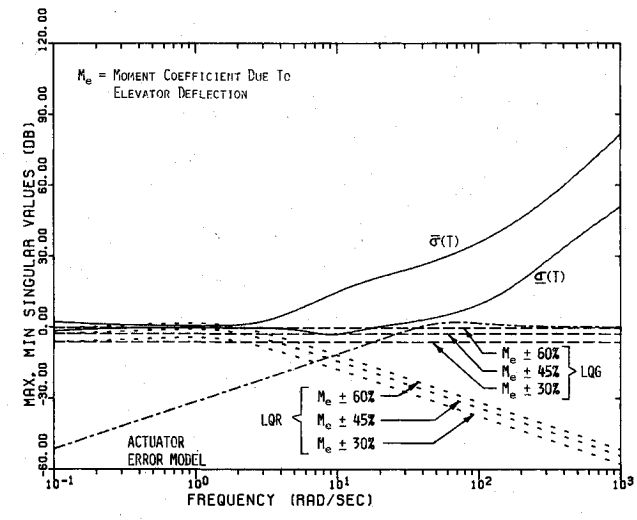

Fig. 5 Singular values of return difference matrix and error models for actuators and parameter variations.

however, behaves as a double integrator at low frequencies and a single integrator at high frequencies. The double integration at low frequencies reflects the compensator structure while the high-frequency rolloff proportional to the inverse of frequency is a characteristic of LQ synthesis.[6] The singular values of the open-loop transfer matrix (loop broken at the plant input) which includes the observer are shown in Fig. 4 for $\beta = 0.5$ (the nominal value), $\beta = 7.07$, and $\beta = 100$. The correspondence between the singular values with $\beta = 0.5$ and $\beta = \infty$ is very good in the midrange frequencies of interest. At low frequencies there is a reduction of tracking performance, but it is of little consequence since the problem time is relatively short. At high frequencies there is a noticeable attenuation inversely proportional to frequency squared. Furthermore, by increasing the observer gain by increasing β according to the Doyle and Stein procedure, the singular values of the open-loop transfer matrix with observer asymptotically approach those of the full-state LQ regulator ($\beta = \infty$). The major limitation in increasing the gain is ensuring that the observer modes satisfy the sampling theorem.

The stability robustness of the present LQG design is demonstrated by the singular value plots of the inverse return difference matrix, Eq. (46), shown in Fig. 5 for $\beta = 0.5$. Note that the largest and smallest singular values at low frequencies are quite close together, with amplitude near one, indicating good tracking performance. This is explicitly shown by the nominal time response in Fig. 2. Also plotted in Fig. 5 are the error models associated with the neglected higher-order actuator dynamics and parameter variations in M_e. The error model singular value $\bar{\sigma}(L_A)$, derived in Sec. V, approaches $\underline{\sigma}(T)$ at high frequencies and limits the bandwidth allowable for the closed-loop system. The error model singular value $\bar{\sigma}(L_p)$ associated with the LQG design is constant over all frequencies. For $\pm 45\%$ and $\pm 60\%$ variations in M_e, condition (47) is violated, and robustness is not guaranteed. Nevertheless, for $\pm 45\%$ variations in M_e, the transient response (Fig. 2) shows little deterioration. Although the singular value plots pertain only to unstructured plant perturbations, the transient responses do reflect the structure of the perturbations and, therefore the transient response for $M_e + 45\%$ is different from that of $M_e - 45\%$.

Note that $\underline{\sigma}(T)$ dips at 10 rad/s. Although a dip remaining above -6 dB is not guaranteed for the LQG regulator, the LQR robustness theory[6] does guarantee that this dip will not be below -6 dB. The fact that no noticeable deterioration occurs shows that the LQG robustness recovery occurs remarkably well in the active frequency region of interest for small values of β (since the controller is only active for about 2 s, very low frequencies are not of interest). Therefore, the LQR singular values of $\underline{\sigma}(T)$ and $\bar{\sigma}(T)$ are not reproduced here. Also plotted in Fig. 5 are the error model singular values for variations in M_e associated with the LQR problem. Here, the gain K_C replaces C in Eq. (53). Note that even though the open-loop transfer matrices converge for $\beta \to \infty$ by Eq. (45), the error models do not. Interestingly, in the low-frequency region, $\bar{\sigma}(L_p)$ for the LQR is slightly above that of $\bar{\sigma}(L_p)$ for the LQG for the same variation in M_e, although in the high-frequency region a $1/\omega$ rolloff occurs such that the $\underline{\sigma}(T)$ is not intersected at its dip. Variations of $\pm 45\%$ are guaranteed stable for the LQR. Finally, the $1/\omega^2$ attenuation at high frequencies due to the observer is desirable over the $1/\omega$ attenuation produced by the LQR (see Fig. 4, $\beta = \infty$).

VII. Conclusions

The application of linear quadratic Gaussian (LQG) synthesis to the design of the multi-input/multi-output (MIMO) longitudinal decoupled mode controller for the AFTI/F-16 is described. The choice of the state space for linear quadratic regulator (LQR) synthesis is tantamount to compensator design in classical control theory. The state space chosen here guarantees zero steady-state tracking under parameter variations. Therefore, this choice of state space results in integral

compensation. The technique that shows that four integrators are required for steady-state tracking is discussed. This procedure also shows that for MIMO systems, adding integrators can result in an uncontrollable state space. The uncontrollable mode is removed by a given linear combination of states.

The choice of weighting matrices in LQR synthesis is seen to be quite important. By a symmetric root locus, the closed-loop roots associated with a diagonal weighting matrix which includes weights on the error rates (in the design state space) produce a wide-band controller. However, nondiagonal weightings on only the errors produce closed-loop roots which induce little interaction with the higher-order actuator dynamics, which are essentially ignored in the controller design. The off-diagonal weightings are effective in shaping the pitch rate response.

Since elevator and flap deflections are not measured directly, an observer based on the Kalman filter formulation is built. The observer gains are chosen so that asymptotically the guaranteed phase and gain margins of full-state feedback are approached. For small values of a key design parameter, the singular values of the LQ loop transfer matrix are very close to those of the LQR in the active frequency region.

Singular value analysis is used to evaluate the robustness of the controller to unmodeled dynamics (the higher-order actuators) and parameter variations. To ensure that desirable time responses also occur (stability analysis is not enough), the system was executed in a linear simulation. For large parameter variations and unmodeled dynamics, little deterioration in performance occurred. There was no effect of sensor noise (with the design variance) on the time responses at the input or output of the plant.

Acknowledgments

The authors appreciate the insights and support given by W. Bennett, R. Toles, J. Watson, and K. Smith of General Dynamics, Fort Worth Division, Dr. M. Desai of the Charles Stark Draper Laboratory, and Professor A. Bryson of Stanford University. This work was supported by General Dynamics, Fort Worth Division.

References

[1]Sain, M., ed., "Special Issue on Multivariable Control," *IEEE Transactions on Automatic Control*, Vol. AC-26, Feb. 1981.

[2]Safonov, M.G. and Athans, M., "Gain and Phase Margin for Multiloop LQG Regulators," *IEEE Transactions on Automatic Control*, Vol. AC-22, April 1977, pp. 173-179.

[3]Lehtomaki, N., Sandell, N., and Athans, M., "Robustness Results in Linear-Quadratic Gaussian Based Multivariable Control Design," *IEEE Transactions on Automatic Control*, Vol. AC-26, Feb. 1981, pp. 75-92.

[4]Safonov, M., Laub, A., and Hartmann, G., "Feedback Properties of Multivariable Systems: The Role and Use of the Return Difference Matrix," *IEEE Transactions on Automatic Control*, Vol. AC-26, Feb. 1981, pp. 47-65.

[5]Kwakernaak, H. and Sivan, R., *Linear Optimal Control Systems*, Wiley-Interscience, New York, 1972.

[6]Doyle, J. and Stein, G., "Multivariable Feedback Design: Concepts for a Classical/Modern Synthesis," *IEEE Transactions on Automatic Control*, Vol. AC-26, Feb. 1981, pp. 4-16.

[7]Athans, M., "On the Design of P-I-D Controllers Using Optimal Linear Regulator Theory," *Automatica*, Vol. 7, Sept. 1971, pp. 643-647.

[8]Brockett, R., *Finite Dimensional Linear Systems*, John Wiley and Sons, New York, 1970.

[9]Bryson, A. and Ho, Y.-C., *Applied Optimal Control*, Blaisdell, Waltham, Mass., 1969.

[10]Bryson, A., "Some Connections Between Modern and Classical Control Concepts," *Transactions of the ASME, Journal of Dynamic Systems, Measurements and Control*, Vol. 101, June 1979, pp. 91-98.

[11]Chen, C., *Introduction to Linear System Theory*, Holt, Rinehart and Winston, New York, N.Y., 1970.

[12]Deckert, J., Desai, M., Deyst, J., and Willsky, A., "F-8 DFBW Sensor Failure Identification Using Analytic Redundancy," *IEEE Transactions on Automatic Control*, Vol. AC-22, Oct. 1977, pp. 795-803.

[13]Athans, M., "The Role and Use of the Stochastic Linear-Quadratic-Gaussian Problem in Control Design," *IEEE Transactions on Automatic Control*, Vol. AC-16, Dec. 1971, pp. 529-552.

[14]Mukhopadhyay, V. and Newsom, J., "Application of Matrix Singular Value Properties for Evaluating Gain and Phase Margin of Multi-loop Systems," *AIAA Guidance and Control Conference*, Aug. 1982, pp. 420-428.

[15]Stein, G. and Doyle, J., "Singular Values and Feedback: Design Examples," *Proceedings of the Allerton Conference*, Montrose, Il., Oct. 1978, pp. 461-470.

[16]Anderson, D.C., Smith, K., and Watson, J.H., "AFTI/F-16 Advanced MULTIMODE Flight Control System Development Concepts and Design," AIAA Paper 82-1571, Aug. 1982.

[17]Smith, K. and Anderson, D.C., "Optimal Control Applications to AFTI/F-16 and Advanced Flight Control System Design," AIAA Paper 82-1572, Aug. 1982.